Hydrochlorofluorocarbon and hydrofluorocarbon emissions in East Asia determined by inverse modeling

A. Stohl[1], J. Kim[2], S. Li[2], S. O'Doherty[3], J. Mühle[4], P. K. Salameh[4], T. Saito[5], M. K. Vollmer[6], D. Wan[7], R. F. Weiss[4], B. Yao[8], Y. Yokouchi[5], and L. X. Zhou[8]

[1]Norwegian Institute for Air Research, Kjeller, Norway [2]School of Earth and Environmental Sciences, Seoul National University, Seoul, Korea [3]School of Chemistry, University of Bristol, Bristol, United Kingdom [4]Scripps Institution of Oceanography, University of California, San Diego, California, U.S.A. [5]National Institute for Environmental Studies, Tsukuba, Japan [6]Swiss Federal Laboratories for Materials Testing and Research (Empa), Duebendorf, Switzerland [7]State Key Joint Laboratory for Environmental Simulation and Pollution Control, Peking University, Beijing, China [8]Centre for Atmosphere Watch and Services, Key Laboratory for Atmospheric Chemistry, Chinese Academy of Meteorological Sciences, Beijing, China

The emissions of three hydrochlorofluorocarbons, HCFC-22 ($CHClF_2$), HCFC-141b (CH_3 CCl_2 F) and HCFC-142b (CH_3 $CClF_2$) and three hydrofluorocarbons, HFC-23 (CHF_3), HFC-134a (CH_2 FCF_3) and HFC-152a (CH_3 CHF_2) from four East Asian countries and the Taiwan region for the year 2008 are determined by inverse modeling.

The inverse modeling is based on in-situ measurements of these halocarbons at the Japanese stations Cape Ochi-ishi and Hateruma, the Chinese station Shangdianzi and the South Korean station Gosan. For every station and every 3 hours, 20-day backward calculations were made with the Lagrangian particle dispersion model FLEXPART. The model output, the measurement data, bottom-up emission information and corresponding uncertainties were fed into an inversion algorithm to determine the regional emission fluxes.

The model captures the observed variation of halocarbon mixing ratios very well for the two Japanese stations but has difficulties explaining the large observed variability at Shangdianzi, which is partly caused by small-scale transport from Beijing that is not adequately captured by the model (Fig. 1).

Based on HFC-23 measurements, the inversion algorithm could successfully identify the locations of factories known to produce HCFC-22 and emit HFC-23 as an unintentional byproduct – however, no information on the factory locations was used in the a priori. The fact that the factory locations could nevertheless be identified lends substantial credibility to the inversion method (Fig. 2).

We report national emissions for China, North Korea, South Korea and Japan, as well as emissions for the Taiwan region in Tables 1-6. Halocarbon emissions in China are much larger than the emissions in the other countries together and contribute a substantial fraction to the global emissions. Our estimates of Chinese emissions for the year 2008 are 65.3±6.6 kt/yr for HCFC-22 (17% of global emissions extrapolated from montzka2009), 12.1±1.6 kt/yr for HCFC-141b (22%), 7.3±0.7 kt/yr for HCFC-142b (17%), 6.2±0.7 kt/yr for HFC-23 (50%), 12.9±1.7 kt/yr for HFC-134a (9% of global emissions estimated from velders2009) and 3.4±0.5 kt/yr for HFC-152a (7%).

Table 1: HCFC-22 emissions (kt/yr) per country/region for the year 2008. B_a and B_b are our best estimate a priori and a posteriori emissions, respectively, based on an inversion with the "best available" a priori information and all data; M_a and M_b are the mean a priori and a posteriori emissions from a suite of 18 different inversions performed, which used different a priori information and data sets. σ_a and σ_b are the corresponding standard deviations.

Country/region	B_a		$M_a \pm \sigma_a$				B_b		$M_b \pm \sigma_b$			
China	79	3	113	9	61	5	65	3	68	1	6	6
Taiwan region	3	0	2	7	1	2	2	5	2	2	0	5
North Korea	0	9	0	8	0	4	2	1	2	2	0	3
South Korea	21	1	18	7	8	3	7	2	7	8	1	4
Japan	7	6	6	7	3	0	6	0	5	9	0	3

Table 2: HCFC-141b emissions (kt/yr) per country/region for the year 2008.

Country/region	B_a		$M_a \pm \sigma_a$				B_b		$M_b \pm \sigma_b$			
China	12	1	16	9	8	9	12	1	12	1	1	6
Taiwan region	1	0	0	9	0	4	0	5	0	5	0	1
North Korea	0	1	0	1	0	1	0	6	0	6	0	1
South Korea	3	1	2	7	1	2	1	8	1	9	0	3
Japan	1	1	1	0	0	4	1	1	1	1	0	1

Table 3: HCFC-142b emissions (kt/yr) per country/region for the year 2008.

Country/region	B_a		$M_a \pm \sigma_a$				B_b		$M_b \pm \sigma_b$			
China	9	6	13	4	7	1	7	3	7	7	0	7
Taiwan region	0	08	0	07	0	03	0	03	0	03	0	01
North Korea	0	11	0	10	0	04	0	20	0	20	0	06
South Korea	2	4	2	2	1	0	0	8	0	8	0	1
Japan	0	7	0	7	0	3	0	6	0	6	0	1

Table 4: HFC-23 emissions (kt/yr) per country/region for the year 2008.

Country/region	B_a		$M_a \pm \sigma_a$				B_b		$M_b \pm \sigma_b$			
China	8	5	8	5	3	5	6	2	6	2	0	7
Taiwan region	0	01	0	01	0	01	0	03	0	02	0	01
North Korea	0	01	0	01	0	01	0	04	0	04	0	02
South Korea	0	27	0	27	0	11	0	19	0	21	0	05
Japan	0	08	0	08	0	03	0	21	0	20	0	03

Table 5: HFC-134a emissions (kt/yr) per country/region for the year 2008.

Country/region	B_a		$M_a \pm \sigma_a$				B_b		$M_b \pm \sigma_b$			
China	20	4	16	3	8	2	12	9	11	9	1	7
Taiwan region	3	2	3	2	1	3	0	8	0	8	0	2
North Korea	0	17	0	19	0	08	0	46	0	47	0	10
South Korea	0	35	0	40	0	18	1	9	1	8	0	3
Japan	3	0	3	0	1	2	3	1	3	1	0	2

Table 6: HFC-152a emissions (kt/yr) per country/region for the year 2008.

Country/region	B_a		$M_a \pm \sigma_a$				B_b		$M_b \pm \sigma_b$			
China	4	0	6	2	3	6	3	4	3	8	0	5
Taiwan region	0	17	0	16	0	07	0	02	0	02	0	02
North Korea	0	17	0	16	0	07	0	15	0	13	0	02
South Korea	0	36	0	34	0	14	0	19	0	21	0	04
Japan	1	6	1	6	0	7	0	9	0	8	0	1

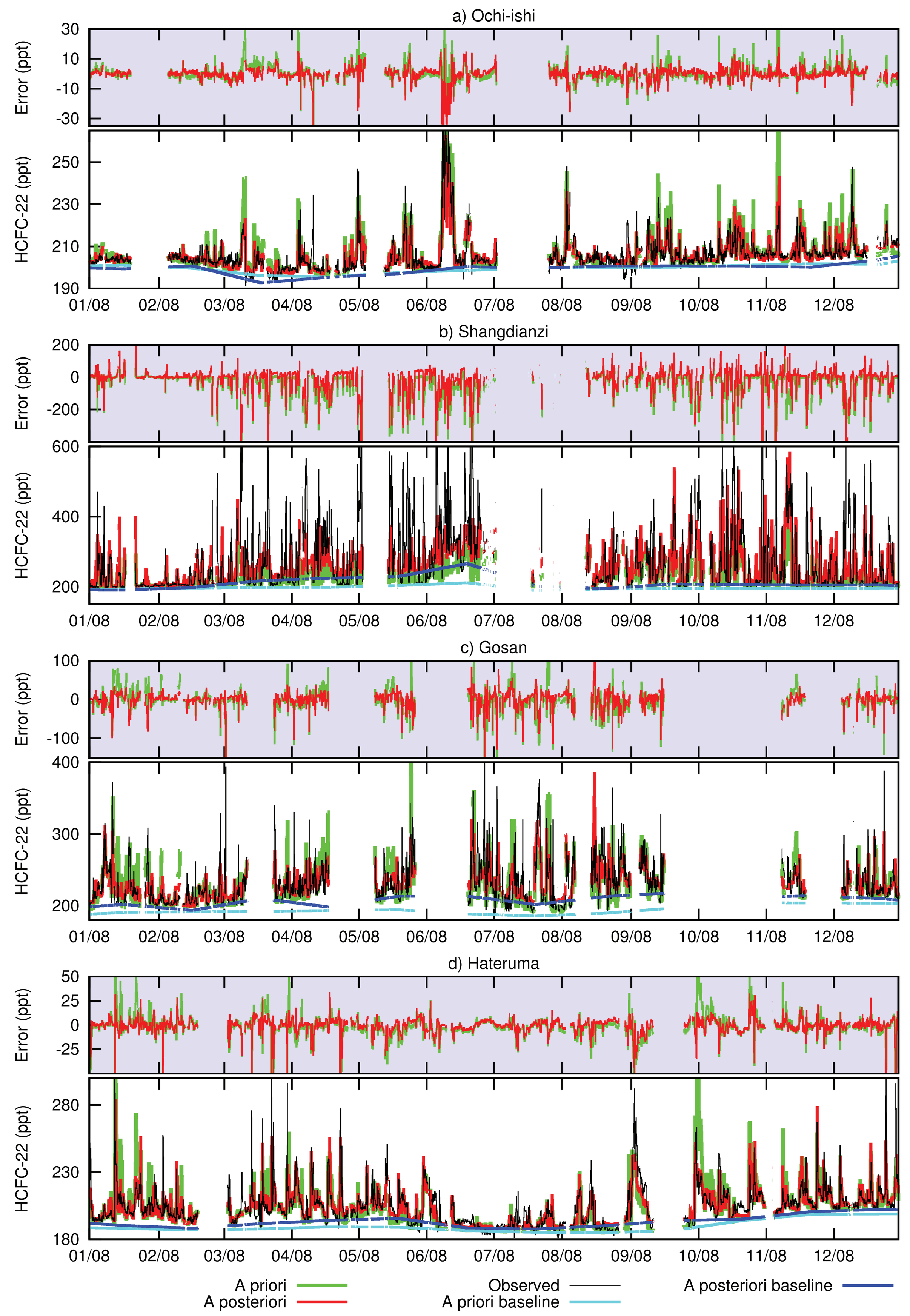

Fig. 2: Maps of the a priori (a), a posteriori (b), and difference between a posteriori and a priori (c) HFC-23 emissions for the year 2008. Black dots indicate the location of measurement stations, asterisks in panels (b) and (c) mark the locations of Chinese and Japanese factories known to have produced HCFC-22 in the year 2008. Notice that although no a priori information on these factories was used, the inversion could find most of the factory locations.

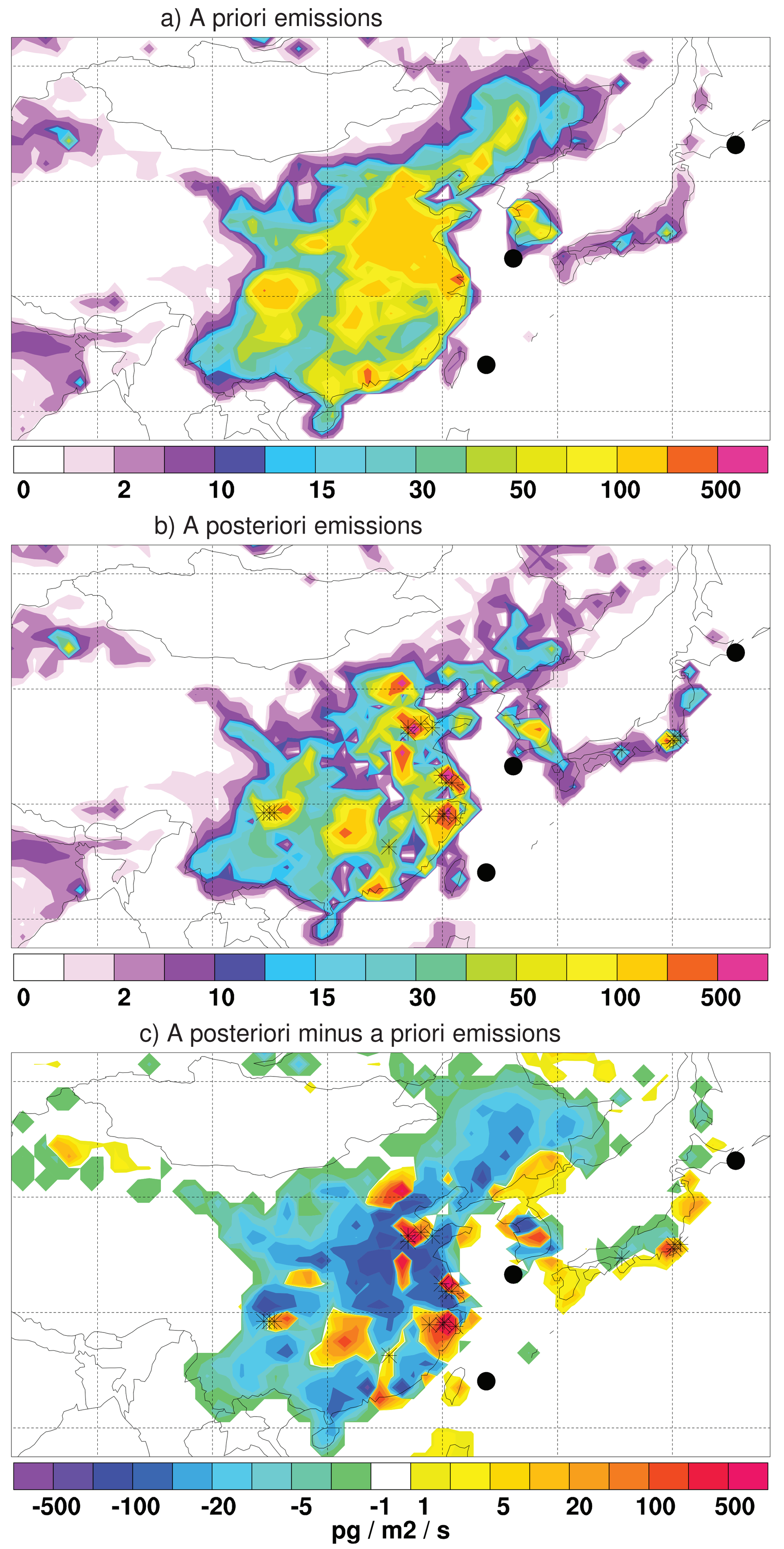

Fig. 1: HCFC-22 time series for a) Ochi-ishi, b) Shangdianzi, c) Gosan, and d) Hateruma. For every station, the lower panels show the observed (black lines) as well as the modeled mixing ratios using the a priori emissions (green lines) and the a posteriori emissions (red lines), the a priori baseline (cyan lines), and the a posteriori baseline (blue lines). The upper panels show the model errors based on the a priori emissions (green lines) and the a posteriori emissions (red lines).